Numerical Study of Atmospheric Ice Accretion on Various Geometric Cross-sections

by

Muhammad S. Virk

REPRINTED FROM

WIND ENGINEERING

VOLUME 35, NO. 5, 2011

MULTI-SCIENCE PUBLISHING COMPANY
5 WATES WAY · BRENTWOOD · ESSEX CM15 9TB · UK
TEL: +44(0)1277 224632 · FAX: +44(0)1277 223453
E-MAIL: mscience@globalnet.co.uk · WEB SITE: www.multi-science.co.uk

Numerical Study of Atmospheric Ice Accretion on Various Geometric Cross-sections

Muhammad S. Virk
High North Technology Centre, Department of Technology, Narvik University College, Norway
Email: msv@hin.no

ABSTRACT
This paper describes the numerical study of atmospheric ice accretion on four different geometric cross sections, *circular, parabola, triangle and cube.* Most structures are the combination of these four basic geometric cross sections. Understanding of the atmospheric ice accretion physics on these will provide a base for further analyses of ice accretion and its effects on complex structures. CFD based numerical analyses are carried out in this research work to understand the rate and shape of atmospheric ice growth on these cross sections. For constant wind speed and atmospheric temperature, the ice growth is simulated as function of time, where more ice accretion is found on cube as compared to three other cross sections. Parametric study to understand the effect of iced surface roughness showed a significant difference in ice growth, when compared with the case, where no surface roughness was assumed on the cross sections.

Keywords: Atmospheric ice, Geometric cross-sections, Surface roughness, Surface temperature, Ice mass.

1. INTRODUCTION
Human activities are increasingly extending to the cold climate regions, where atmospheric icing will not only create human inconveniences, but will also affect human activities especially in the construction industry (communication towers and ski lifts), energy distribution (power network cables and towers), maritime activities, aviation conditions on the ground, meteorological observations and wind energy power production. Various structures such as power network cables, telecommunication masts etc have been damaged or destroyed on numerous occasions due to the added mass of ice or an increase in aerodynamic interaction leading to unacceptable movements [1]. Detailed knowledge of frequency and duration of icing events as well as maximum ice loads are crucial parameters for the design of structures in cold regions.

Atmospheric icing on structures occurs in conditions, where the cooling of an air mass causes the super cooling of the water droplets. Water droplets in the earth atmosphere can remain in the liquid state at air temperature as low as –40°C, before spontaneous freezing occurs [2, 3]. The rate of atmospheric ice accretion on a structure is governed by two processes; the impingement of super cooled water droplets on the structure surface and the surface thermodynamics, which determines that what portion of the water impingement freezes or on other hand melts previously accreted ice. Numerical study of atmospheric ice accretion on structures includes the computation of mass flux of icing particles as well as determination of the icing conditions [4]. This can be numerically simulated by means of integrated thermo-fluid dynamic models, which requires the use of various numerical tools in order to obtain the aerodynamics flow field, the particle behavior, surface thermodynamic and phase change. Most developments in the numerical modeling of ice accretion are focused on aerospace industry and very few improvements have been reported in the research field of structural icing. Various numerical studies related to the atmospheric icing on structures can be found in literature. The first attempts were made from late 1970's to obtain data from simulating ice shapes on structures, where researchers such as Ackley and Templeton [5], Lozowski and Oleskiw [6–8], McComber et al. [9, 10], Smith and Barker [11] has concentrated on understanding the physical ice accretion processes and developing numerical models to predict the severity of icing on structures. During 1990's Makkonen [12, 13], Finstad et al. [14], Shin et al. [15–17] & Skelton et al. [18] worked on numerical modeling of the atmospheric ice accretion on various types of structures. Most of these efforts were focused on the aerospace structures and power network cables.

This paper describes the numerical study of atmospheric ice accretion on four basic geometric cross sections, *circular, parabola, triangle and cube*, where each cross section had a constant radius of 5 mm. The analyses were carried out at dry rime ice conditions, for T = –10 °C. Ice accretion on each cross section in this study was analyzed by making a comparison of droplet collision efficiency, ice mass, ice thickness and surface temperature distribution. Most structures are the combination of these basic cross sections, therefore understanding of atmospheric ice accretion physics on these will provide a base for further analyses of ice accretion on the complex shape structures.

2. NUMERICAL SETUP

The numerical analyses were carried out using a finite element based Navier Stoke equation solver 'FENSAP-ICE' from NTI [19]. The primary advantage of finite element based method is its ability to model complex shaped boundaries, where the size and shape of the finite element can be varied allowing the greater accuracy. C-type structured, numerical grid was used for each cross section, where as to accurately determine the boundary layer characteristics (shear stresses and heat fluxes), a $y+$ value less than 1 was used near the wall of each cross section. The sand grain roughness height for the iced surface was calculated with an empirical NASA correlation [17]. Two phase flow (air & water) was solved using Eulerian-Eulerian approach, where super cooled water droplets were assumed to be spherical. The main advantage of using Eulerian-Eulerian approach is that, the same mesh can be used for multiphase flow calculations and ice geometry.

The Eulerian two phase fluid model consists of the Navier-Stokes equation, augmented by the water droplets continuity and momentum equation. The water droplet drag coefficient is based on the empirical correlation for the flow around the spherical droplets described by Clift et al. [20]. Mono-dispersed droplet size distribution was assumed for the numerical analyses. Surface thermodynamic and icing rate are calculated by using the mass and energy conservation equations, considering the heat fluxes due to convective cooling, evaporative cooling, latent heat of fusion, viscous heating and kinetic heating. Jones formulae for the ice density calculation was used for these analyses. ALE (Arbitrary Langrangian Eulerian) formulation was used for the mesh displacement due to ice accretion in time. This approach adds the grid speed terms to the Navier-Stokes equations to account for the mesh velocity [21]. The numerical simulations were carried out at the operating conditions specified in Table 1.

Table 1: Operating conditions used for the simulations.

Free Stream Wind Velocity [m/s]	10
Droplet Size, MVD [μm]	35
Liquid Water Content, LWC [g/m^3]	1.0
Atmospheric Air Temperatures [°C]	−10
Simulation Time [minutes]	30

3. AIRFLOW AND DROPLET BEHAVIOR

Air flow field around each cross section was numerically simulated by solving the incompressible Navier Stokes equations. Numerical analyses of the air flow behavior showed a change in the velocity and pressure distribution along each geometric cross section. For circular and parabolic cross sections streamlines followed the object and no high flow separation was observed, where as for cube and triangular shape cross sections more complex flow behavior was observed, where high flow separations zones exist at downstream side. Such flow behavior affects the aerodynamics and convective heat transfer during the ice accretion process. Figure 1 shows the velocity distribution and streamlines along each cross section.

Two phase flow (air & water) was simulated using Eulerian-Eulerian approach, where water droplets, MVD = 35 μm, were assumed to be spherical. Numerical analyses showed a difference in the droplet behavior and collision efficiency for each cross section. Parabolic cross section has the highest value of collision efficiency, where as the triangular had the lowest one, but surface area analyses of each cross section showed that cube had the highest possibility of droplet collision, whereas circular cross section had the lowest one. Figure 2 shows the droplet collision efficiency and location for each cross section. Most droplets collide at the windward side of the cross sections, where as for cube and triangular cross sections, droplets also hit at upper, lower and leeward side of the cross sections. Such behavior of droplet collision location affects the surface heat transfer due to latent heat of fusion and droplet kinetic energy during the ice accretion process.

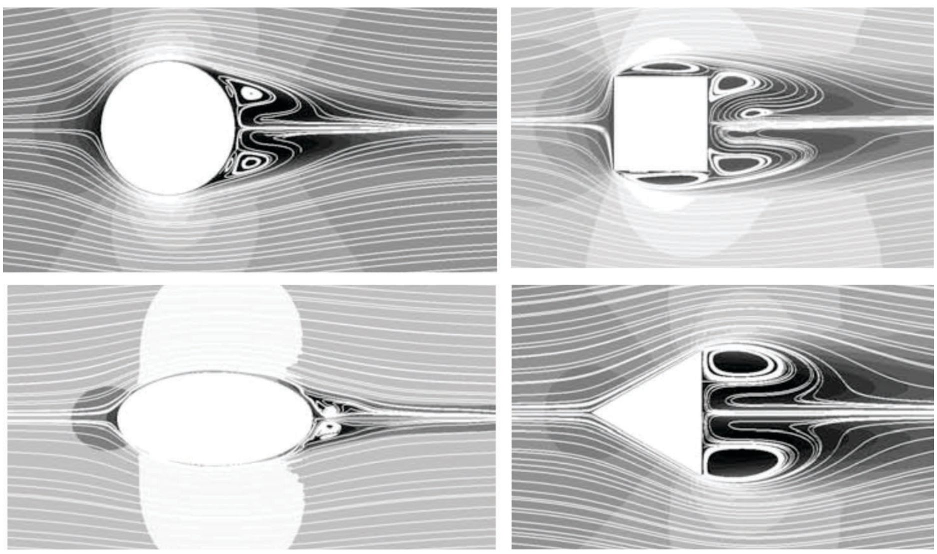

Figure 1: Velocity distribution and streamline behavior around each cross section.

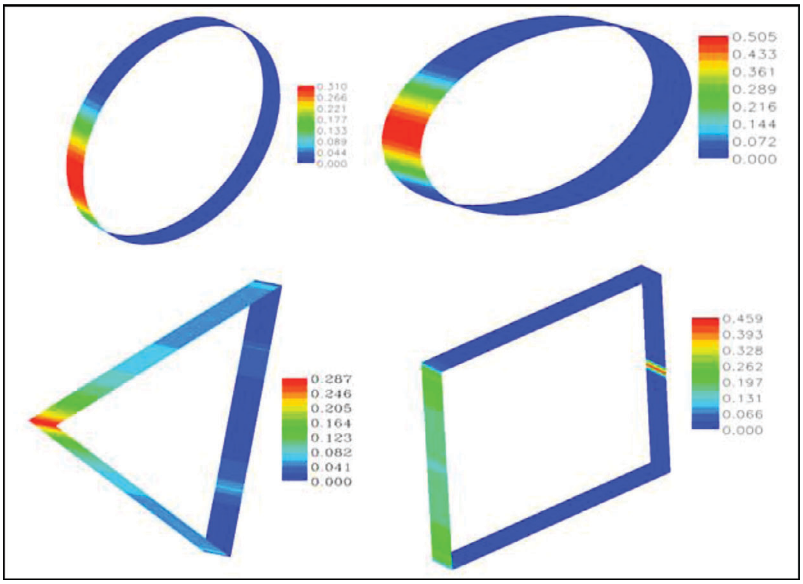

Figure 2: Droplet collision efficiency on each cylindrical cross section.

4. ATMOSPHERIC ICE ACCRETION

To numerically study the rate and shape of atmospheric ice accretion on each cross section, analyses were carried out for $t = 30$ minutes, where each time step was $\Delta t = 0.0001$ sec. Figure 3 shows the atmospheric ice growth on each cross section. Numerical results of icing rate and location is found to be in good agreement with the trends of droplet collision efficiency and its location on each cross sectional surface. The rate of ice accretion is found to be high at the locations of high droplet collision efficiency on each cross section's surface. For circular and parabolic cross sections ice accretion is mainly occurred at windward side, where as for cube and triangular cross sections, ice accretion is also found on top, bottom and leeward side of the cross sections. This difference in ice accretion location is mainly due to difference in air flow and droplet behavior across each surface. As an overall results showed the maximum atmospheric ice accretion on the cube cross section, which is mainly due to more surface area hit by the droplets. Figure 3 shows the rate and shape of atmospheric ice growth on each cross section for $t = 30$ minutes.

To further study and understand the ice growth on these geometric cross sections, detailed analyses were carried out, where different parameters such as droplet collision efficiency, surface temperature, ice thickness and ice growth distribution along each cross section surface was studied. Figure 4 shows the results of these analyses. Droplet collision is the most important parameter in this regard, as it determines the possible locations and frequency of ice accretion on every cross section surface. Results showed that although parabolic shape had the highest value of droplet collision efficiency, but area wise analyses of each cross section surface showed that cube surface had the highest rate of droplet collision. Distribution of droplet collision efficiency along each surface showed that for circular and parabolic cross sections, very small area come in contact with the droplets, most of the droplets only hits at front side of these cross sections, where as for cube and triangle more surface area is hit by the droplets, which also increased the area covered by the ice on cube and triangle. Due to water droplet collision with the surface, the latent heat is released by the droplets that are transferred to the each cross section surface, which increases the surface temperature at the point of droplet collision.

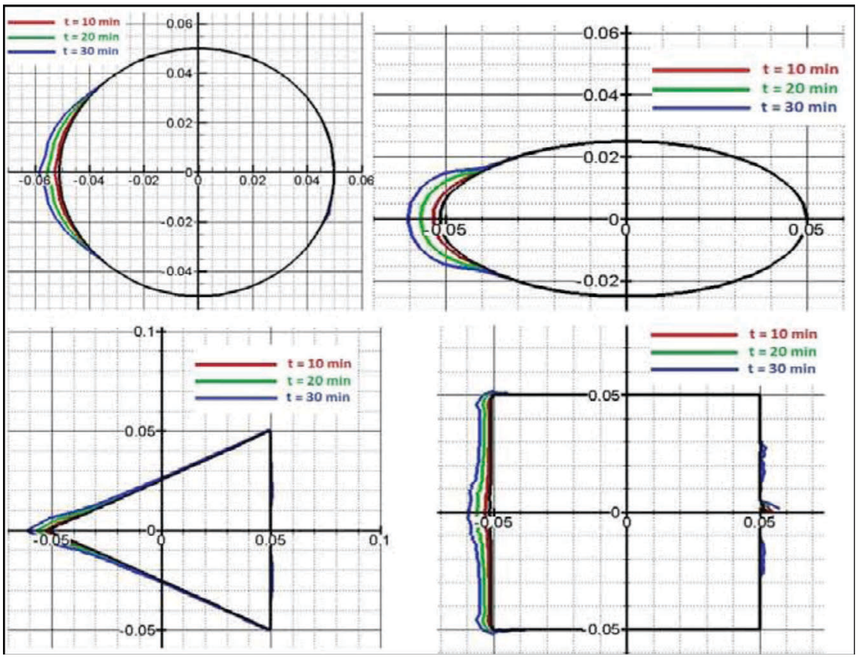

Figure 3: Rate and shape of atmospheric ice growth on each cross section.

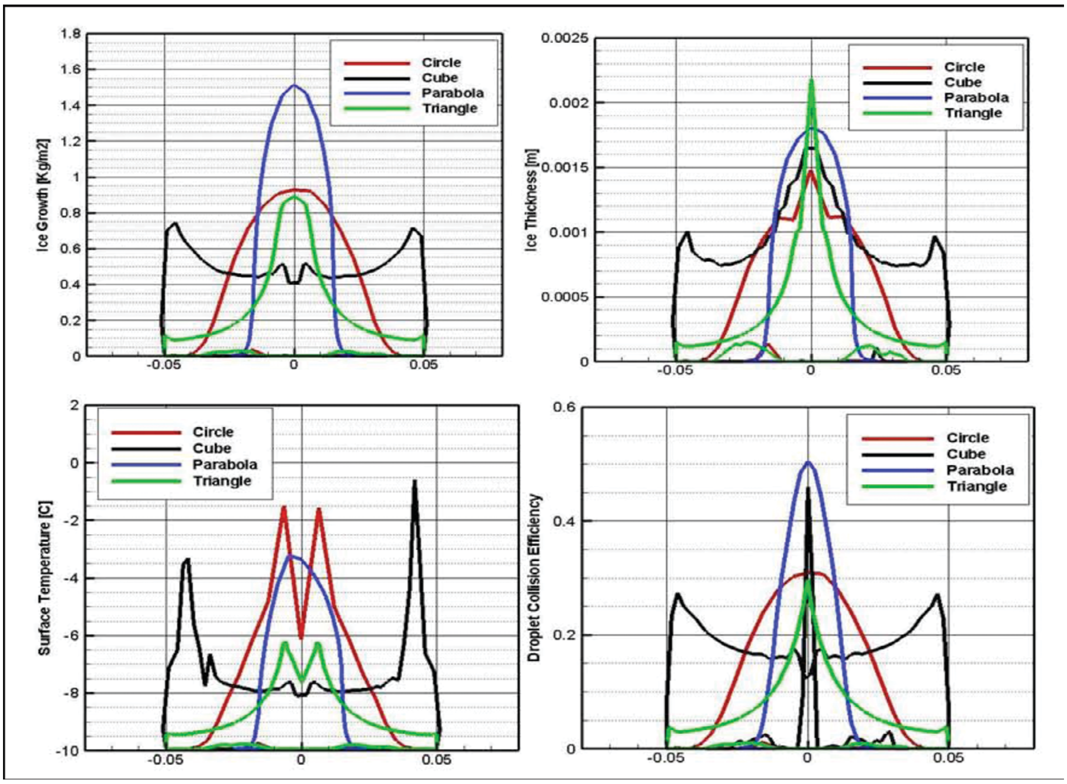

Figure 4: Analyses of ice growth on each cross section.

Heat balance during the ice accretion process is mainly the combination of the aerodynamic heating from the compression of the flow, the kinetic energy of the droplet impact, the latent heat released by the droplet freezing and the heat loss in warming the super-cooled droplets to 0 °C. Due to more droplet collision and complex flow behavior in

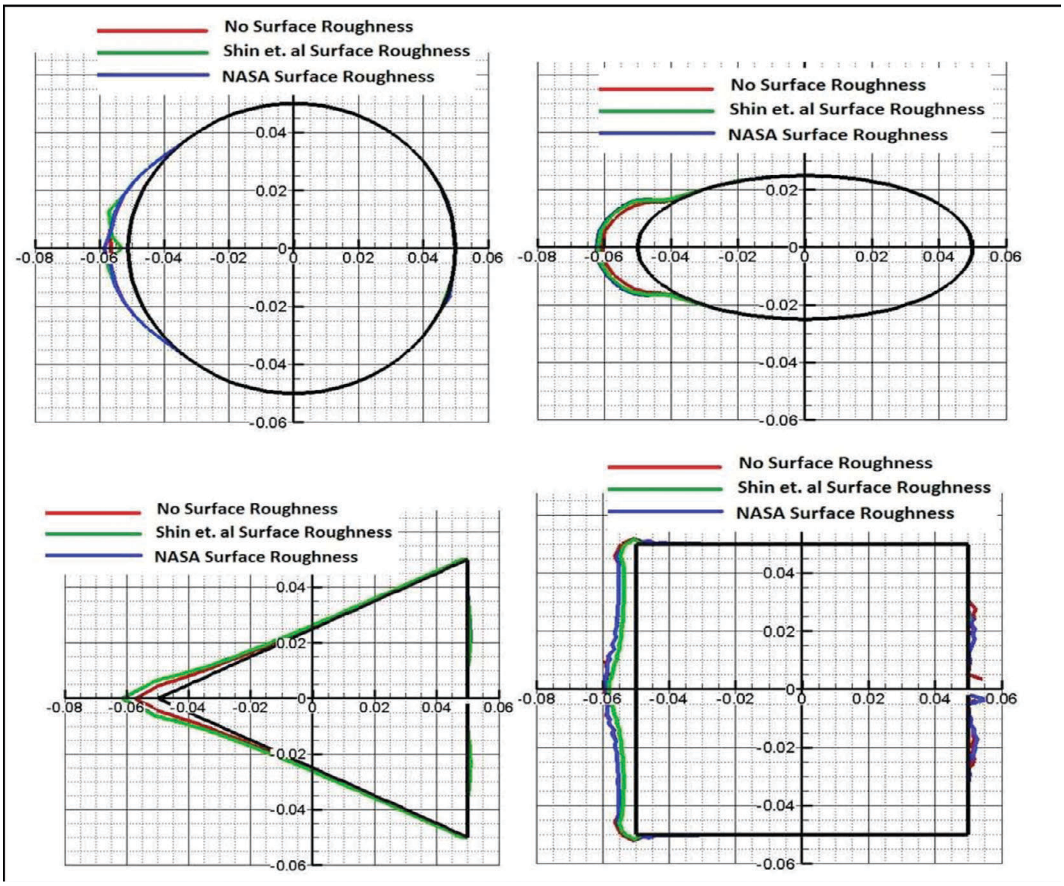

Figure 5: Effect of iced surface roughness on ice accretion.

case of cube, high values of heat transfer due to aerodynamics heating and latent heat of fusion is observed even at the corners of the cube, which leads to an increase in the ice accretion. Results showed that although parabolic cross section has the highest value of ice thickness and growth, but area wise analyses showed that cube surface area has the highest values.

5. EFFECT OF ICED SURFACE ROUGHNESS MODEL

Iced surface roughness occurs during the initial stages of the ice accretion process, before any ice starts to accrete. Shin et al. [15] found that three main zones evolve in the ice accretion process on a surface, the smooth zone, rough zone and the feather zone. The roughness elements are bluff bodies with 3D separation behind each element with the characteristic length of the separation on the order of the roughness size. The element drag and the separation govern the effect the roughness had on the surface flow field and the boundary layer development. For this study two different numerical models, NASA surface roughness & Shin et.al, of iced surface roughness was analyzed and compared with a case of no surface roughness, to analyze their effect on rate and shape of ice growth on these geometric cross sections. All the analyses were carried for the operating conditions specified in Table 1. Figure 5 shows the rate and shape of atmospheric ice growth for each surface roughness case on each cross section. Results showed a difference in ice growth, when a comparison was made between no surface roughness and the surface roughness case, but no significant difference was found between NASA surface roughness & Shin et.al surface roughness model ice growth.

6. CONCLUSIONS

A CFD based numerical study has been presented in this paper to understand and analyze the rate and shape of atmospheric ice accretion on four different geometric cross sections. Numerical analyses provided a base to understand the ice accretion process on each geometric cross section. For constant wind speed, and temperature the atmospheric ice growth is simulated as function of time. As an overall results showed more ice accretion on cube cross section, when compared with circle, parabola and triangular cross sections. Parametric study to understand the effect of iced surface roughness showed a significant difference in ice growth, when compared with the case, where no surface roughness was assumed, but no significant difference was found between NASA surface roughness & Shin et.al surface roughness model ice growth.

ACKNOWLEDGMENT

The work reported in this paper was partially funded by the Research Council of Norway, project no. 195153/160 and partially by the consortium of the project ColdTech- Sustainable Cold Climate Technology.

REFERENCES

1. T G Myers and J.P.F. Charpin., *A mathematical model for atmospheric ice accretion and water flow on a cold surface.* Heat & Mass Transfer, 2004. **47**: p. 5483–5500.
2. Kathleen F Jones and K.Z. Egelhofer, *Computer model of atmospheric ice accretion on transmission lines.*
3. Battan, I.J., *Cloud physics and cloud shedding.* 1962, New York: Doubledayand Co.
4. T Wagner, U. PEil, and C. Borri, *Numerical investigation of conductor bundle icing,* in *EACWE 5.* 2009: Florence, Italy.
5. S F Ackely and M.K. Templeton., *Computer modelling of atmopsheric ice accretion.* 1979, USA cold region research and engineering labortory.
6. E P Lozowski, J R Stallabrass, and F.P. Hearty., *The Icing of anunheated, Non-rotating Cylinder, Part I: A Simulation Model.* Journal of Climate and Applied Meteorology, 1983. **22**: p. 2053–2062.
7. E P Lozowski and M.M. Oleskiw, *Computer modelling of time dependant rime icing in the atmosphere.* 1983, USA cold regions research and engineering labortory.
8. E P Lozowski, K J Finstad, and E.M. Gates, *Comments on calculation of the impingement of cloud droplets on a cylinder by finite element method.* Journal of atmospheric science, 1985. **42**(3): p. 306–307.
9. McComber, P. *Numerical simulation of ice accretion on cables.* in *First international workshop on Atmospheric icing on structures.* 1983. Haniver, Hampshire.
10. McComber, P., R Martin, and G. Morin. *Estimation of combined ice and wind loads on overhead transmission lines.* in *First international workshop on atmospheric icing on structures.* 1983. Hanover, Hampshire.
11. B W Smoth and C.P. Barker. *Icing of cables.* in *First international workshop on atmospheric icing on structures.* 1983. Hanover, Hampshire.
12. Makkonen, L, *Models for the growth of rime, glaze, icicles and wet snow on structures.* Philosiphical transactions of the Royal Society A, 2000. **358**(1776): p. 2913–2939.
13. Makkonen, L, T. Laakso, and M. Marjaniemi, *Modelling and prevention of ice accretion on wind turbines.* Wind Engineering, 2001. **25**(1): p. 3–21.

14. Finstad, Lozowski, and Gates, *A computational investigation of water droplet trajectories.* Journal of atmospheric and ocenic technologies, 1988. **5**: p. 160–170.

15. Shin, J., *Prediction of ice shapes and their effect on airfoil drag.* Journal of aircraft, 1994. **31**(2): p. 263–270.

16. Boutanios, Z., *An Eulerian 3D analysis of water droplets impingement on a Convair-580 nose and cockpit geometry,* in *Department of Mechanical Engineering.* 1999, Concordia University, Canada: Montreal.

17. J Shin and T.H. Bind., *Experimental and computational ice shapes and resulting drag increase for a NACA 0012 airfoil.* 1992, NASA technical memorandum 105743.

18. Skelton and Poots, *Snow accretion on overhead line conductors of finite torsional stiffness.* Cold region science and technology, 1991. **19**: p. 301-316.

19. http://www.newmerical.com/index.php/products/fensap-ice-cfd-software/.

20. R Clift, J R Grace, and M.E. Weber, *Bubbles, Drops and Particles.* 1978, New York: Academic Press.

21. Manual, N.S.U. 2010, NTI.